

Description of five larvae of the genus *Gnaptorina* Reitter, 1887 from Xizang, China (Coleoptera, Tenebrionidae, Blaptinae), with molecular species delimitation and diagnoses

Bao-Yue Ji¹, Tong-Yang Guo¹, Mei-Chang Gu¹, Guo-Dong Ren¹, Xiu-Min Li¹

¹ Key Laboratory of Zoological Systematics and Application of Hebei Province, College of Life Sciences, Institute of Life Science and Green Development, Hebei University, Baoding 071002, China

Corresponding author: Xiu-Min Li (lixiumin@hbu.edu.cn)

Abstract

With 39 described species in three subgenera, the *Gnaptorina* is the second most species-rich genus in the subtribe Gnaptorinina (Tenebrionidae: Blaptinae). In this study, a phylogeny of *Gnaptorina* was reconstructed based on one nuclear (28S-D2) and three mitochondrial (COI, Cytb, and 16S) gene fragments; multiple molecular species delimitation approaches were also implemented to assess the taxonomic status of larval specimens based on COI gene fragment. Larvae of five known species of the subgenus *Hesperoptorina* are described and illustrated for the first time: *Gnaptorina nigera* Shi, Ren & Merkl, 2007, *Gnaptorina tishkovi* Medvedev, 1998, *Gnaptorina brucei* Blair, 1923, *Gnaptorina himalaya* Shi, Ren & Merkl, 2007, *Gnaptorina kangmar* Shi, Ren & Merkl, 2007. A key to larvae of four genera of the tribe Blaptini and a key to the known larvae of the genus *Gnaptorina* are provided. This study provides valuable morphological data for larval studies of the tribe Blaptini.

Key words: Beetles, Gnaptorinina, immature stage, morphology, species identification



Academic editor: Patrice Bouchard
Received: 29 March 2024
Accepted: 9 July 2024
Published: 14 August 2024

ZooBank: <https://zoobank.org/D45D45AB-9525-4911-825D-900982CFE71C>

Citation: Ji B-Y, Guo T-Y, Gu M-C, Ren G-D, Li X-M (2024) Description of five larvae of the genus *Gnaptorina* Reitter, 1887 from Xizang, China (Coleoptera, Tenebrionidae, Blaptinae), with molecular species delimitation and diagnoses. ZooKeys 1209: 295–314. <https://doi.org/10.3897/zookeys.1209.124184>

Copyright: © Bao-Yue Ji et al.
This is an open access article distributed under terms of the Creative Commons Attribution License ([Attribution 4.0 International – CC BY 4.0](https://creativecommons.org/licenses/by/4.0/)).

Introduction

The Gnaptorinina Medvedev, 2001 is a species-rich subtribe of Blaptini Leach, 1815, consisting of 189 species in 12 genera: *Agnaptorina* Reitter, 1887 (36 species and subspecies), *Asidoblaps* Fairmaire, 1886 (56 species), *Blaptogonia* Medvedev, 1998 (five species), *Colasia* Koch, 1965 (seven species), *Gnaptorina* Reitter, 1887 (39 species and subspecies), *Itagonia* Reitter, 1887 (24 species and subspecies), *Montagona* Medvedev, 1998 (three species), *Nepalindia* Medvedev, 1998 (five species), *Pseudognaptorina* Kaszab, 1977 (four species), *Sintagona* Medvedev, 1998 (one species), *Tagonoides* Fairmaire, 1886 (eight species), and *Viattagona* Medvedev & Merkl, 2003 (one species) (Medvedev and Merkl 2002; Medvedev 2004; Ren et al. 2016; Li et al. 2018, 2019; Chigray 2019; Iwan and Löbl 2020; Bai et al. 2020, 2023; Ji et al. 2024). With 39 described species, *Gnaptorina* is the second most species-rich genus in the subtribe Gnaptorinina. The genus *Gnaptorina* is currently subdivided into three subgenera: *Gnaptorina* Reitter, 1887, *Austroptorina* Bai, Li & Ren, 2020, and *Hesperoptorina* Medvedev, 2009 (Medvedev 2009; Li et al. 2021). To date, immature stages

of six species in three genera are described within Gnaptorinina: *Gnaptorina* Reitter, 1887 (larvae of three species), *Agnaptorina* Reitter, 1887 (larvae of two species) and *Itagonia* Reitter, 1887 (larva of one species) (Yu et al. 1996, 1999; Medvedev 2006; Zhu and Ren 2014; Ji et al. 2024). Larval morphology is important for understanding the systematics of different groups, and it has been used to support the close relationships of genera (Grebennikov and Scholtz 2004; Lawrence et al. 2011; Kamiński et al. 2019), including for supraspecific classification of the tribe Blaptini (Skopin 1960; Chigray and Kirejtshuk 2023). However, the larvae were described for only a few species of Blaptini.

In this study, we constructed a molecular phylogenetic tree for the genus *Gnaptorina* and a molecular species delimitation, combining them to verify the taxonomic status of larval specimens. These larvae belong to the five known species of the subgenus *Hesperoptarina* of the genus *Gnaptorina*. Larvae of these five species are described and illustrated. The present results will enrich the existing mitochondrial gene library of the tribe Blaptini and lay the foundation for future evolutionary study of the endemic insects on the Qinghai-Xizang Plateau.

Materials and methods

Morphological examination

In total, 170 larval samples of five species were examined for this study, which are deposited at the Museum of Hebei University, Baoding, China (**MHBU**). The larvae used for the description above were inferred to be in their older instar stage based on previous research on the larval biology of the Blaptini.

The photos were taken with the following imaging system: (a) Canon EOS 5D Mark III (Canon Inc., Tokyo, Japan) connected to a Laowa FF 100 mm F2.8 CA-Dreamer Macro 2× or Laowa FF 25 mm F2.8 Ultra Macro 2.5–10× (Anhui Changgeng Optics Technology Co., Hefei, China). (b) A Leica M205A stereomicroscope equipped with a Leica DFC450 camera (Leica Microsystems, Singapore) was controlled using the Leica application suite v. 4.3; (c) JVC KY-F75U (JVC Kenwood, Long Beach, CA, USA) digital camera attached to a Leica Z16 APO dissecting microscope (Leica Microsystems, Buffalo Grove, IL, USA) with an apochromatic zoom objective and motor focus drive, using a Syncroscope Auto-Montage System (Synoptics, Cambridge, UK) and software. Multiple images were stacked to construct the final figures. Photographed specimens were illuminated with either an LED ring light attached to the end of the microscope column, with incidental light filtered to reduce glare, or by a gooseneck illuminator with bifurcating fibreoptics; image stacks were white-balance corrected using the system software (Synoptics, Cambridge, UK). Montaged images were edited using Adobe Photoshop v. 22.1.0 to form the final figure plates.

Label data are presented verbatim. A slash (/) separates text on different lines of label.

Taxon sampling, DNA extraction, PCR amplification, and sequencing

Larval specimens were collected in the field from Xizang, China. To correlate the different stages, the molecular data were obtained from larval individuals.

DNA was extracted from pygopod tissue of the larva using the Insect DNA Isolation Kit (BIOMI-GA, Hangzhou, China) following the manufacturer's protocols. The DNA extracted was stored at -20 °C. Fragment of mitochondrial molecular marker (cytochrome oxidase subunit I, COI) was amplified with the primers F 2183 and R 3014 (Folmer et al. 1994). The profile of the PCR amplification consisted of an initial denaturation step at 94 °C for 4 min, 35 cycles of denaturation at 94 °C for 45 s, annealing at 47 °C for 1.5 min, an extension at 72 °C for 1 min, and a final 8 min extension step at 72 °C. PCR was performed using TaKaRa Ex Taq (TaKaRa, Dalian, China). PCR products were subsequently checked by 1% agarose gel electrophoresis and sequencing was performed at General Biol Co. (Anhui, China). Finally, we obtained five sequences for five larvae. Detailed information for the new samples in this study is provided in Table 1.

Table 1. List of larvae examined in this study with the corresponding accession number.

Species	Sampling locality	Elevation (m)	Date of collection	Collector(s)	Accession number
<i>G. nigera</i>	Damxung County, Xizang, China (XZDX)		23.VII.2014	G. Ren et al.	PQ013187
<i>G. tishkovi</i>	Qomolangma, Tingri County, Xizang, China (XZDR)	4960	20.VII.2023	X. Bai et al.	PQ013187
<i>G. brucei</i>	Tingri County, Xizang, China (XZDR)	4820	28.VII.2014	G. Ren et al.	PQ013185
<i>G. kangmar</i>	Gyangzê County, Xizang, China (XZJZ)		6.VIII.2014	G. Ren et al.	PQ013184
<i>G. himalaya</i>	Qusum County, Xizang, China (XZSN)	4790	31.VII.2019	X. Li et al.	PQ013185

Phylogenetic analyses

In total, we used 306 sequences from 88 individuals, including 301 published sequences (from 81 adults, one larva, one pupa) and five new sequences from larvae (Li et al. 2021; Ji et al. 2024). We used the previously published sequences of two species of Platyscelidini Lacordaire, 1859 as outgroups, which have been considered as close relatives of the tribe Blaptini (Kamiński et al. 2021).

The phylogenetic tree was constructed based on concatenated datasets of mitochondrial and nuclear DNA sequences (COI, Cytb, 16S, and 28S-D2) by Maximum Likelihood (ML). A best-fit model was tested according to the corrected Akaike's Information Criterion (AIC) using ModelFinder (included in IQ-TREE) with the software PhyloSuite v. 1.2.2 (Zhang et al. 2020). The ML tree search was performed in IQ-TREE v. 1.6.8 (Nguyen et al. 2015) that was also plugged into PhyloSuite. The ML tree was inferred using an edge-linked partition model for 5000 ultrafast bootstraps (1000 replicates) (Minh et al. 2013). Support for each node is represented by ultrafast bootstrap values (uBV).

Molecular species delimitation analyses

Recent studies have shown that some molecular species definition methods may underestimate or overestimate the number of species (Dellicour and Flot 2018; Luo et al. 2018). Hence, it has been advocated to use them in a complementary way to better assess species boundaries. Here, we used a combination of three distinct methods (ASAP, GMYC, and PTP) to assess the boundaries of species within *Gnaptorina*.

We relied on the Assemble Species by Automatic Partitioning (ASAP) approach as implemented on the online web application (<https://bioinfo.mnhn>).

fr/abi/public/asap/asapweb.html, Puillandre et al. 2021). ASAP analysis was carried out based on COI gene fragment, and outgroups were excluded. In addition to the distance-based ASAP method, we also performed tree-based analyses using two distinct methods: the General Mixed Yule Coalescent (GMYC) model and Poisson-tree-processes (PTP) (Pons et al. 2006; Zhang et al. 2013). Accordingly, GMYC analysis was conducted on an ultrametric tree from the BEAST analysis, with all outgroups removed. The analysis was conducted in R using the package GMYC with default settings (100 trees randomly selected, 250 million generations with a burn-in of 25 million and a thinning parameter of 100). PTP analysis relied on the best-score ML tree from the IQ-TREE analysis and was carried out on the web server of the Exelixis Lab (<http://species.h-its.org/ptp/>) using default settings.

Results

Phylogenetic relationships and species delimitation

The final, the IQ-TREE analysis yielded a topology based on concatenated dataset (2219 bp), including 306 sequences from 88 individuals (Fig. 1). The individuals of *Gnaptorina* were grouped into three well-supported clades: C1 (*Gnaptorina*, uBV = 76), C2 (*Austroptorina*, uBV = 100), and C3 (*Hesperoptorina*, uBV = 79). The monophyly of each subgenus was supported overall.

The ML tree and three molecular species delimitation methods associate the larvae and adults of different species with consistent results. Larva and known species cluster into a single well-supported clade respectively (uBV = 100). Three molecular species delimitation results showed that the samples XZDX01, XZDR02, XZDR03, XZJZ04, and XZSN05 consistently merged individuals from known species. Therefore, we conclude that the above assumption is correct: the sample XZDX01 is the larva of *G. nigera*, the sample XZDR02 is the larva of *G. tishkovi*, the sample XZDR03 is the larva of *G. brucei*, the sample XZJZ04 is the larva of *G. kangmar*, and the sample XZSN05 is the larva of *G. himalaya*.

Key to larvae of four genera of the tribe Blaptini

- 1 Epipharynx with six mastoids above the basal spines2
- Epipharynx with eight mastoids above the basal spines..... ***Itagonia***
- 2 Urogomphi conspicuous.....3
- Urogomphi inconspicuous..... ***Gnaptorina***
- 3 Labrum with not less than 6 setae on apical part***Blaps***
- Labrum with less than 6 setae on apical part ***Prosodes***

Larval diagnosis of the genus *Gnaptorina* Reitter, 1887

The last segment is conical in shape; urogomphi are inconspicuous and the apex is truncated; body is brownish yellow, shiny, with ossified body wall and midline is distinct (Yu et al. 1999). Pairs of setae grow on each tergum. Labrum is transverse; apical part with six setae; anterior margin with two discal setae and lateral margin with sparse setae. Clypeus is trapezoidal, with two pairs of setae at apex and margin, respectively. Epicranial stem is Y- or V-shaped.

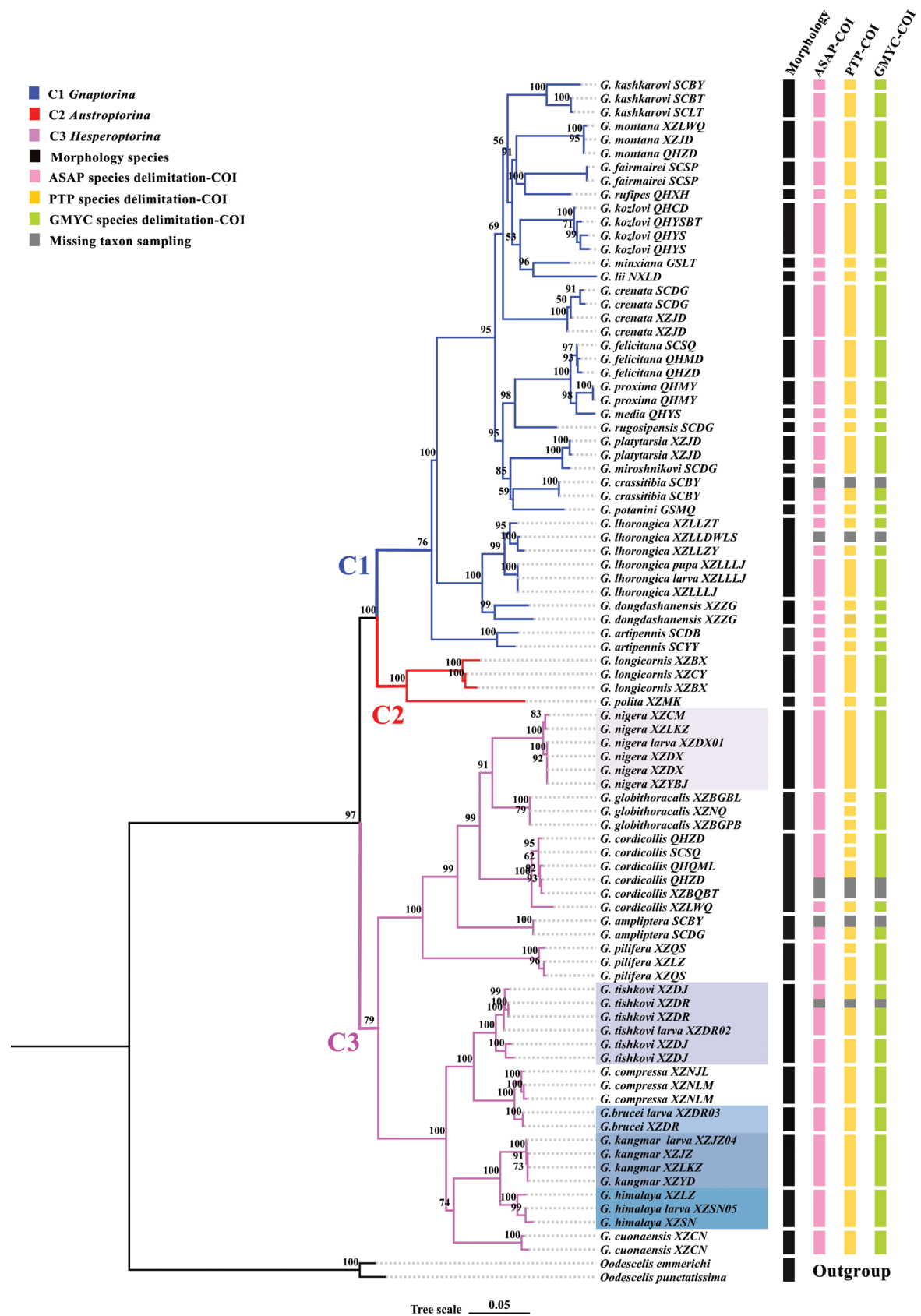


Figure 1. Maximum-likelihood phylogenetic tree based on 2219 bp of mitochondrial and nuclear DNA sequences (COI, Cytb, 16S, and 28S-D2) within the genus *Gnaptorina*. Vertical coloured bars delineate extant morphospecies (black), and the results of three separate molecular analyses delimiting species (pink, yellow, and pale green). For the analysis using COI gene, we used grey colour to delineate specimens for which sequencing failed.

Mandible membranous elevation with two setae. Maxillary palpi are three-segmented, with a seta inside and outside anterior margin of II. Labial palpi are two-segmented, prementum with two setae apically, mentum and submentum with sparse setae. Antennae are three-segmented, the apex of II is dilated and baseball-like, sensation circle C-shaped at apex of II, III is cylindrical, much narrower and shorter than I and II. Prothoracic leg is noticeably stronger, longer, and thicker than meso- and metathoracic legs; each tarsus has differentiated into a highly ossified tarsungulus and a weakly ossified base, with one seta internally at base and one short thick spine laterally; inner margin of each segment with a row of pectinate setae.

Key to the species of known larvae of the genus *Gnaptorina*

- 1 Mentum trapezoidal (Fig. 2A).....2
- Mentum elongate hexagonal (Fig. 2B).....3
- 2 Median line obvious on pro- and mesonotum.....*G. kangmar*
- Median line obvious on thorax dorsally and abdominal tergite I ... *G. himalaya*
- 3 Ocelli evident (Fig. 2C)4
- Ocelli inconspicuous (Fig. 2D).....7
- 4 Antennal segment I longer than II5
- Antennal segment I shorter than II.....*G. cylindricollis*
- 5 Submentum with 10 setae.....*G. felicitana*
- Submentum with 6 setae.....6
- 6 Median line obvious on thorax dorsally*G. nigera*
- Median line obvious on thorax dorsally and abdominal tergite I *G. tishkovi*
- 7 Mentum with 2 setae*G. lhorongica*
- Mentum with 12 setae*G. brucei*

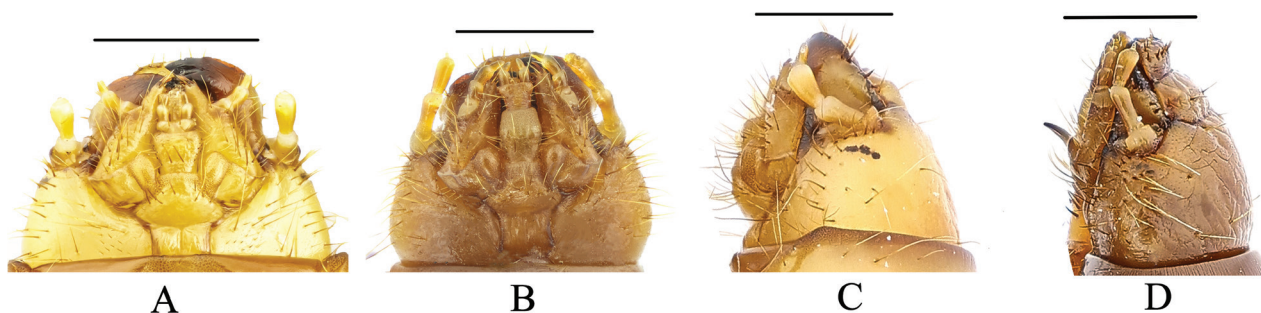


Figure 2. **A** head of *Gnaptorina himalaya*, ventral view **B** head of *G. brucei*, ventral view **C** head of *G. himalaya*, lateral view **D** head of *G. brucei*, lateral view. Scale bars: 1 mm.

Descriptions of larvae

Gnaptorina nigera Shi, Ren & Merkl, 2007

Examined materials. Larvae. 3 exx. (MHB): Damxung County, Xizang/ 30°16.05' N, 90°42.60' E/ Alt. 4480 m/ 2023-VII-9/ Xiu-Min Li, Tong-Yang Guo leg.; 20 exx. (MHB): Damxung County, Xizang/ 30°20.78' N, 91°03.58' E/ Alt. 4150m/ 2019-VIII-8/ Xiu-Min Li leg.; 31 exx. (MHB): Yangbajain Township, Damxung County, Xizang/ 2014-VII-23/ Guo-Dong Ren, Xing-Long Bai, Jun-Sheng Shan leg.; 4 exx. (MHB): Damxung County, Xizang/ 30°32.32' N, 91°06.42' E/ Alt. 4350m/

2019-VIII-9/ Xiu-Min Li leg.; 11 exx. (MHBU): Chamda Township, Nagarzê County, Xizang/ 29°00.48' N, 91°04.87' E/ Alt. 4540m/ 2019-VIII-8/ Xiu-Min Li leg.; 11 exx. (MHBU): Comai County, Xizang/ 28°50.92' N, 91°22.57' E/ Alt. 4490m/ 2023-VII-8/ Xiu-Min Li leg.; 6 exx. (MHBU): Daglung Township, Nagarzê County, Xizang/ 28°39.48' N, 90°28.10' E/ Alt. 4615m/ 2014-VIII-6/ Guo-Dong Ren, Xing-Long Bai, Jun-Sheng Shan leg.

Description. Body (Fig. 3A–C). Larvae length 17.2–17.5 mm, width 2.1–2.5 mm. Body subcylindrical; last segment conical; body brownish yellow, shiny, body wall ossified; median line obvious on thorax dorsally; pairs of setae grow on each tergum.

Head (Fig. 3E, D–G). Prognathous, slightly narrower than width of prothorax; labrum transverse; apical part with six setae; anterior margin with two discal and six slender lateral marginal setae; epipharynx with sparse setae on lateral margin, with two basal spines on central area, between the basal spines with four mastoids, with six mastoids above the basal spines (Fig. 3G); mandible left-right unsymmetrical, membranous elevation with two setae; clypeus transverse, trapezoidal, dark brown, with two pairs of setae at apex and margin respectively (Fig. 3D, F). Epicranial stem Y or V-shaped; frons convex, dark brown throughout, with sparse long setae on lateral margins, with four pairs of setae at apex (a pair on anterior margin, a pair on middle margin, two pairs on posterior margin) (Fig. 3D, F). Ocelli evident, two parallel rows arranged transversely (Fig. 3B). Maxillary palpi (Fig. 3E) three-segmented, cylindrical, and conical at apex; I widest, II longest, I as long as III. Labial palps two-segmented, short; II conical;

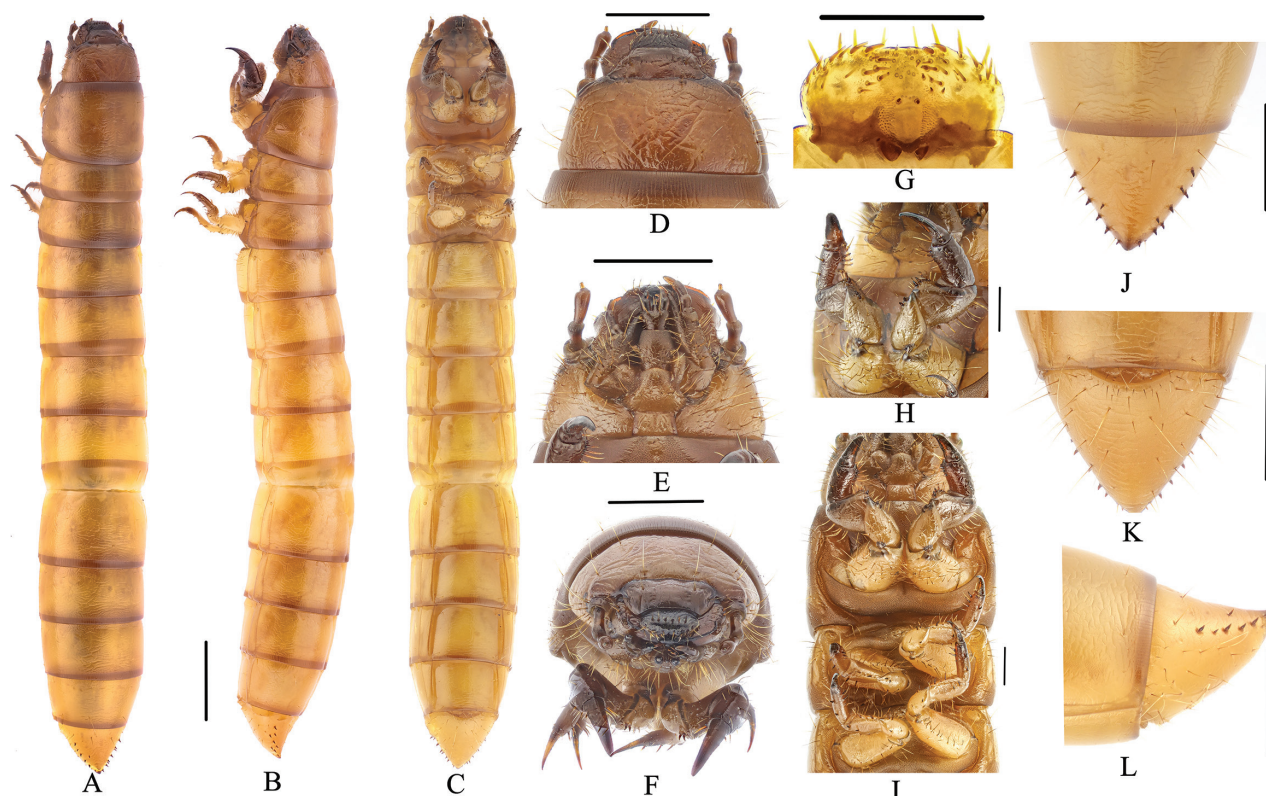


Figure 3. Larva of *Gnaptorina nigera* Shi, Ren & Merkl, 2007 **A** habitus, dorsal view **B** habitus, lateral view **C** habitus, ventral view **D** head, dorsal view **E** head, ventral view **F** head, vertex view **G** epipharynx **H** prothoracic leg **I** legs **J** pygopods, dorsal view **K** pygopods, ventral view **L** pygopods, lateral view. Scale bars: 2 mm (A–C); 1 mm (D–F, J–L); 0.5 mm (G, H, I).

prementum with two setae on anterior margin, apex with two long setae, lateral sides with four or five long setae; mentum convex, hexagonal, base of mentum straight; mentum more slender than prementum, lateral margins with four or five long setae, posterior margin with four setae; submentum with six setae on mid-posterior part (three on left, three on right). Antennae three-segmented, cylindrical at apex; I longest, as wide as II; III shortest and narrowest (Fig. 3B, D–F).

Thorax (Fig. 3A). Thoracic segments parallel-sided, with transverse plicae. Pronotum and mesonotum with two pairs of elongate setae on anterior and posterior margin. Metanotum with two pairs of setae on anterior margin and a pair of setae on posterior margin. Anterior and posterior border of pronotum with brown longitudinal stripes, with pair of irregular brown spots on tergum, posterior border of mesonotum and metanotum with a brown longitudinal stripe. Pronotum longest, $2.40 \times$ as long as mesonotum, $1.70 \times$ as long as metanotum, mesonotum shortest.

Legs (Fig. 3H, I). Protarsungulus strongly sclerotised, sharp, claw-like; protarsungulus with a strong, long seta on inner side and a strong, short spine on outer side at base. Profemora and protibiae gradually narrowing towards apex; inner margin setal formula of prothoracic leg 4(3): 6(3): 2(2); outer margin of tibiae with two setae; outer margin of femora with two setae; trochanter with two setae (Fig. 3G). Mesotarsus with a strong, long seta on inner side and a strong, short spine on outer side at base; inner margin setal formula of mesothoracic leg 3–4(2–3): 4(2): 2(2); outer margin of tibiae with two spines; outer margin of femora with two spines; outer margin of trochanters with two spines. Metatarsus with two short, broad spines at base, inner margin setal formula of metathoracic leg 3(2): 4(2): 2(2), outer margin of tibiae with two short spines, outer margin of femora with two spines, outer margin of trochanters with two spines. Meso- and metathoracic legs shorter than prothoracic one, meso- and metathoracic legs tarsungulus highly ossified, hooked, with dense setae (Fig. 3I).

Abdomen (Fig. 3C, J–L). Approximately $3.10 \times$ as long as thorax; abdominal segments I–VIII subcylindrical, with transverse plicae; ventral side of abdominal segment I with six pairs of setae on each side (five pairs of setae near anterior and a pair of setae near posterior) and 14 setae on anterior margins, ventral side of abdominal segments II–VIII with three pairs of setae on anterior, middle, and posterior margin of lateral margins, respectively (Fig. 3C). Last segment conical, $0.91 \times$ as long as VIII, distinctly narrower than VIII; surface of convex disc with sparse long setae in ventral view, with a row of short spines on each side (six spines on left, seven spines on right); last segment dorsally flattened; urogomphi inconspicuous and apex truncated, with two short spines (Fig. 3J–L).

Spiracles (Fig. 3C). Lateral margins of abdominal segments I–VIII and mesothorax each with a pair of spiracles, mesothoracic spiracles much larger than abdominal one, lateral margins of abdominal segments I–VIII with almost equal-sized spiracles, rounded.

***Gnaptorina tishkovi* Medvedev, 1998**

Examined materials. Larvae. 14 exx. (MHBU): Qomolangma, Tingri County, Xizang/ $28^{\circ}11.33'$ N, $86^{\circ}49.80'$ E/ Alt. 4960m/ 2023-VII-20/ Xing-Long Bai, Quan-Yu Ji, Jian Song leg.; 5 exx. (MHBU): Tingri County, Xizang/ $28^{\circ}36.68'$

N, 87°07.78' E/ Alt. 4270m/ 2014-VII-24/ Guo-Dong Ren, Xing-Long Bai, Jun-Sheng Shan leg.; 5 exx. (MHBU): Tingri County, Xizang/ 28°27.58' N, 87°37.15' E/ Alt. 4480m/ 2019-VIII-16/ Xiu-Min Li leg.; 10 exx. (MHBU): Dinggyê County, Xizang/ 28°08.48' N, 87°42.45' E/ Alt. 4700m/ 2014-VIII-4/ Guo-Dong Ren, Xing-long Bai, Jun-Sheng Shan leg.; 5 exx. (MHBU): Dinggyê County, Xizang/ 2014-VIII-4/ Guo-Dong Ren leg.

Description. Body (Fig. 4A–C). Larvae length 21.8–23.5 mm, width 2.4–3.0 mm. Body yellowish brown, shiny, body wall ossified; median line obvious on on thorax dorsally and abdominal tergite I.

Head (Fig. 4B, D–G). Labrum transverse; apical part with six setae; anterior margin with two discal and six slender lateral marginal setae; epipharynx with sparse setae on lateral margin, with two basal spines on central area, between the basal spines with four mastoids, with six mastoids above the basal spines (Fig. 4G); mandible left-right unsymmetrical, membranous elevation with two setae (Fig. 4D, F). Epicranial stem Y-shaped, epicranial stem with a pair of pale brown patterns on distal margin; frons convex, with sparse long setae on lateral margins, with four pairs of setae at apex (a pair on upper margin, a pair on middle margin, two pairs on mid-posterior margin) (Fig. 4D, F). Posterior margin of middle part of frontal pale brown covered. Ocelli evident (Fig. 4B). Maxillary palpi (Fig. 4E) three-segmented, cylindrical, and conical at apex; I widest, II longest. Labial palps two-segmented, short; II conical; prementum with two setae on anterior margin, apex with two long setae, lateral sides with two long setae; mentum convex, hexagonal; mentum more slender than prementum, posterior margin with four long setae; submentum with six setae on posterior margin (three on left, three on right). Antennae three-segmented, cylindrical at apex; I longest and widest; III shortest and narrowest (Fig. 4B, D–G).

Thorax (Fig. 4A). Pronotum and metanotum with two pairs of elongate setae on anterior margin and a pair of setae on posterior margin. Mesonotum with a pair of setae on anterior, middle, and posterior margin. Anterior and posterior borders of pronotum with brown longitudinal stripes, posterior border of mesonotum and metanotum with a brown longitudinal stripe. Pronotum longest, 1.96 × as long as mesonotum, 1.61 × as long as metanotum, mesonotum shortest.

Legs (Fig. 4H). Protarsungulus with a strong, long seta on inner side and a strong, short spine on outer side at base. Profemora and protibiae gradually narrowing towards apex; inner margin setal formula of prothoracic leg 3–4(1–2):6(3):2(2); outer margin of tibiae with two strong, short spines; outer margin of femora with two setae; trochanter with two short setae. Mesotarsus with a strong, long seta on inner side and a strong, short spine on outer side at base; inner margin setal formula of mesothoracic leg 4:5(1):2(2); outer margin of tibiae with two spines; outer margin of femora with two spines; outer margin of trochanters with two spines and one seta. Metatarsus with a strong, long seta on inner side and a strong, short spine on outer side at base; inner margin setal formula of metathoracic leg 3–4(2):4(3):2(2), outer margin of tibiae with two spines, outer margin of femora with two spines, outer margin of trochanters with two spines and one seta.

Abdomen (Fig. 4A, C). Not constricted between VIII and IX segments. Approximately 4.20 × as long as thorax; abdominal segments I–VIII

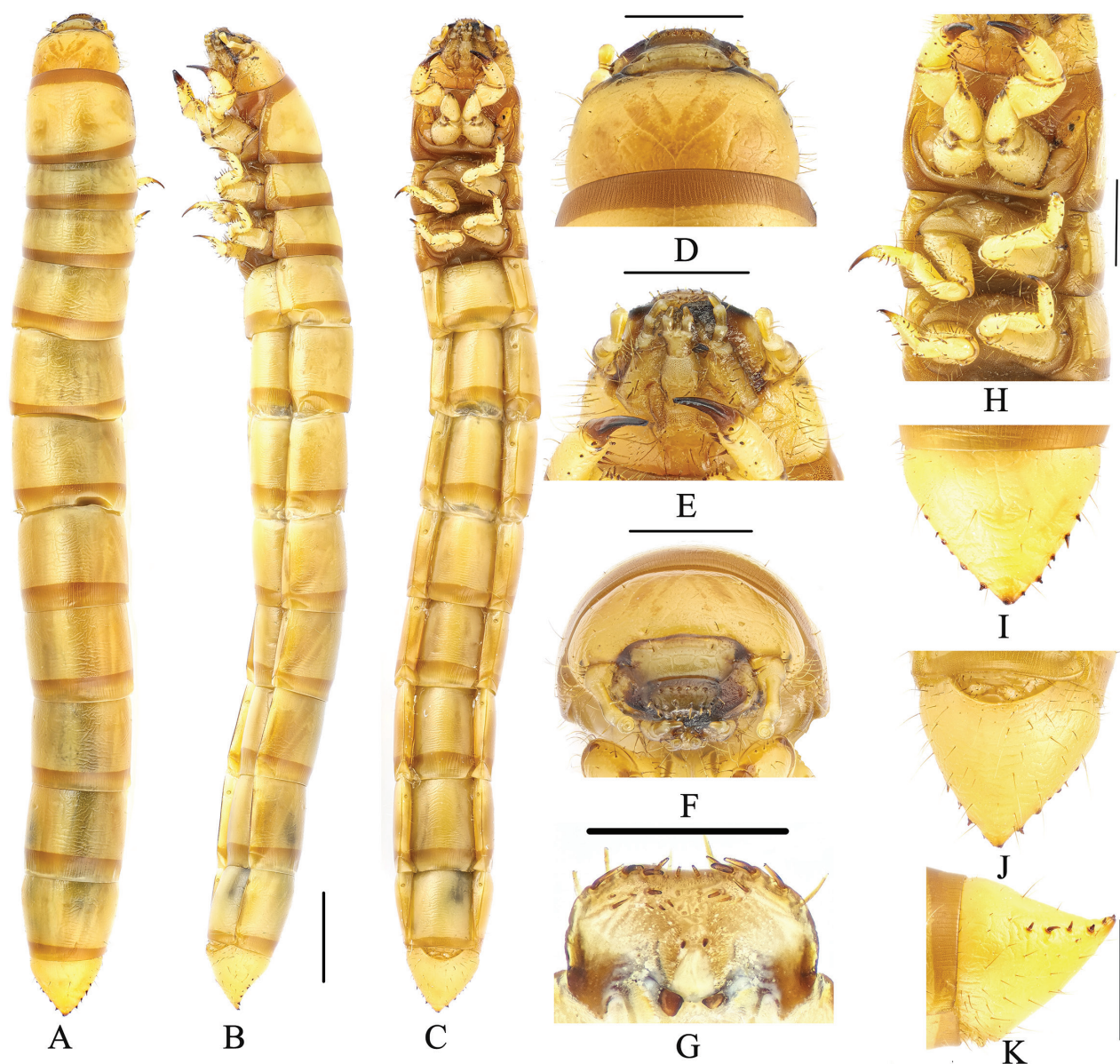


Figure 4. Larva of *Gnaptorina tishkovi* Medvedev, 1998 **A** habitus, dorsal view **B** habitus, lateral view **C** habitus, ventral view **D** head, dorsal view **E** head, ventral view **F** head, vertex view **G** epipharynx **H** legs **I** pygopods, dorsal view **J** pygopods, ventral view **K** pygopods, lateral view. Scale bars: 2 mm (**A–C**); 1 mm (**D–F, H–K**); 0.5 mm (**G**).

subcylindrical, with transverse plicae; ventral side of abdominal segment I with sparse setae on anterior and lateral margins, with four setae on posterior margin (two on left, two on right); ventral side of abdominal segments II–VIII with three pairs of setae on anterior, middle, and posterior margin of lateral margins, respectively. Last segment conical, $0.87 \times$ as long as VIII, distinctly narrower than VIII; surface of convex disc with sparse long setae in ventral view, with a row of short spines on each side (six spines each on left and right); last segment dorsally flattened; urogomphi inconspicuous and apex truncated, with two short spines (Fig. 4I–K).

Spiracles (Fig. 4C). Mesothoracic spiracles are almost twice size of abdominal segment I spiracles; lateral margins of abdominal segments I–VIII and mesothorax each with a pair of oval spiracles, abdominal segment I spiracles largest, abdominal segments I–VIII spiracles gradually shrinking.

***Gnaptorina brucei* Blair, 1923**

Examined materials. Larvae. 2 exx. (MHBU): Rongxar Township, Tingri County, Xizang/ 28°10.92' N, 86°29.25' E/ Alt. 4820m/ 2014-VII-28/Guo-Dong Ren, Xing-Long Bai, Jun-Sheng Shan leg.

Description. Body (Fig. 5A–C). Larvae length 24.5–25.5 mm, width 2.2–2.5 mm, comparatively thin. Body yellowish brown, shiny, body wall ossified; median line obvious on thorax dorsally and abdominal tergite I.

Head (Fig. 5B, D–H). Labrum transverse; apical part with six setae; anterior margin with two discal and six slender lateral marginal setae; epipharynx with sparse setae on lateral margin, with two basal spines on central area, between the basal spines with four mastoids, with six mastoids above the basal spines (Fig. 5H); mandible left-right unsymmetrical, membranous elevation with two setae (Fig. 5D, E). Epicranial stem Y-shaped; frons convex, frons with densely long setae on lateral margins, with four pairs of setae at apex (a pair on anterior margin, a pair on mid-anterior margin, two pairs on mid-posterior margin) (Fig. 5D). Ocelli inconspicuous (Fig. 5B). Maxillary palpi (Fig. 5E) three-segmented, cylindrical, and conical at apex; I widest, II longest. Labial palps two-segmented, short; II conical; prementum with two setae on anterior margin, apex with two long setae, lateral sides with four long setae; mentum convex, hexagonal; mentum more slender than prementum, lateral margin with five or six long setae, posterior margin with one long setae; submentum with eight setae on posterior margin. Antennae three-segmented, cylindrical at apex; I longest and widest; III shortest and narrowest.

Thorax (Fig. 5A). Each thoracic tergum with two pairs of elongate setae on anterior and posterior margin. Anterior and posterior borders of pronotum with brown longitudinal stripes; posterior border of mesonotum and metanotum with a brown longitudinal stripe. Pronotum longest, 1.70 × as long as mesonotum, 1.45 × as long as metanotum, mesonotum shortest.

Legs (Fig. 5I). Protarsungulus with a strong, long seta on inner side and a strong, short spine on outer side at base. Profemora and protibiae gradually narrowing towards apex; inner margin setal formula of prothoracic leg 5(3): 6–7(4): 2(2); outer margin of tibiae with one short seta and one strong, short spine; outer margin of femora with two setae; trochanter with three setae. Mesotarsus with a strong, long seta on inner side and a strong, short spine on outer side at base; inner margin setal formula of mesothoracic leg 3(3): 5(3): 2(2); outer margin of tibiae with two spines; outer margin of femora with two spines; outer margin of trochanters with one spine and two setae. Metatarsus with a strong, long seta on inner side and a strong, short spine on outer side at base; inner margin setal formula of metathoracic leg 3(2): 5–6(3): 2(2), outer margin of tibiae with two spines, outer margin of femora with two spines, outer margin of trochanters with one spine and two setae.

Abdomen (Fig. 5A, C). Constricted between VIII and IX segments. Approximately 3.54 × as long as thorax; abdominal segments I–VIII subcylindrical, with transverses plicae; ventral side of abdominal segment I with sparse setae on anterior and lateral margins, with two setae on posterior margin; ventral side of abdominal segments II–VIII with two pairs of setae on lateral margin. Last segment conical, 0.79 × as long as VIII, distinctly narrower than VIII; last segment surface of convex disc with sparse long setae in ventral view, with a row

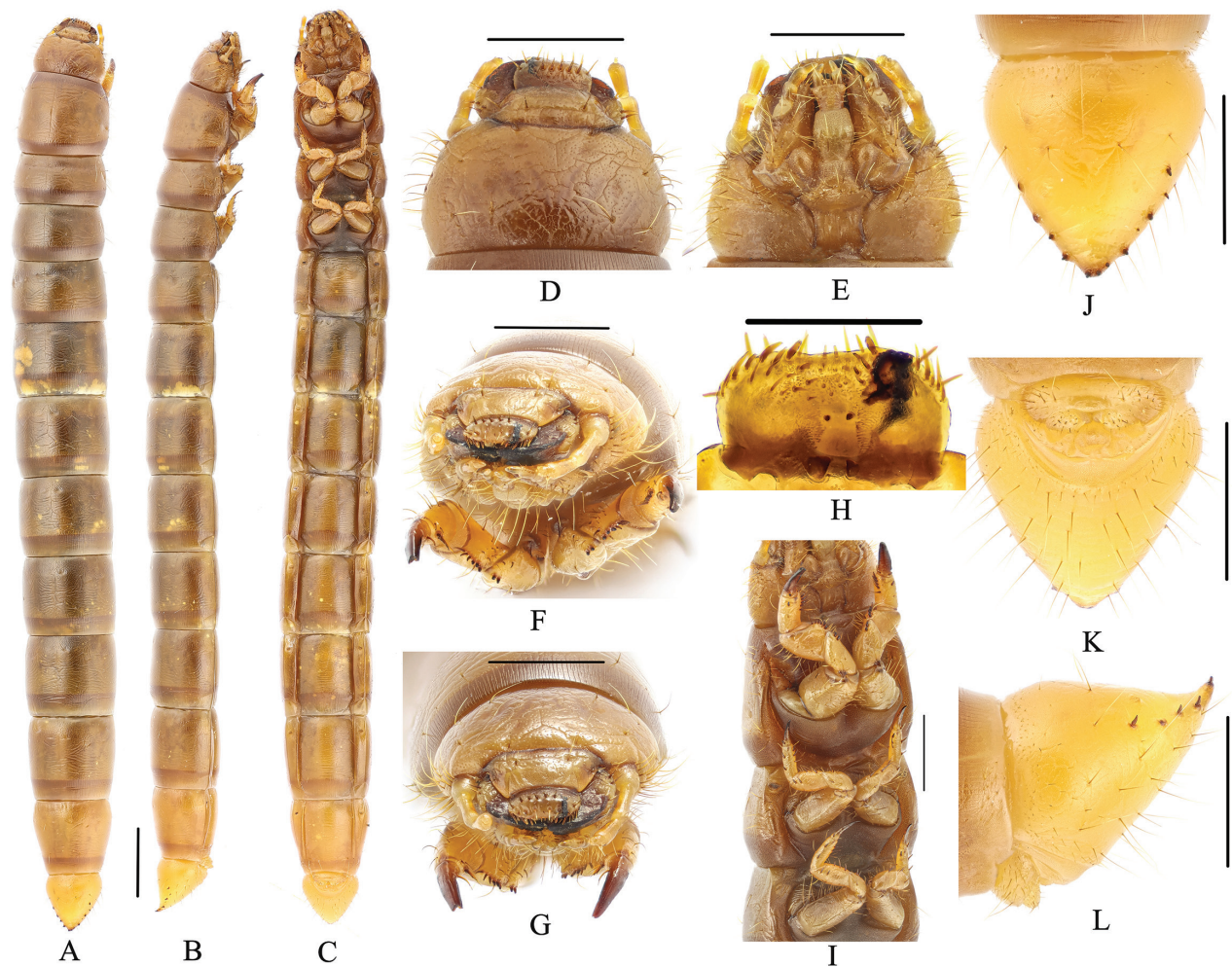


Figure 5. Larva of *Gnaptorina brucei* Blair, 1923 **A** habitus, dorsal view **B** habitus, lateral view **C** habitus, ventral view **D** head, dorsal view **E** head, ventral view **F, G** head, vertex view **H** epipharynx **I** legs **J** pygopods, dorsal view **K** pygopods, ventral view **L** pygopods, lateral view. Scale bars: 2 mm (**A–C**); 1 mm (**D–G, I–L**); 0.5 mm (**H**).

of short spines on each side (four spines on left, six spines on right); urogomphi inconspicuous and upturned slightly, with two short spines (Fig. 5J–L).

Spiracles (Fig. 5C). Lateral margins of abdominal segments I–VIII and mesothorax each with a pair of oval spiracles, mesothoracic spiracles largest, abdominal segments I–VIII spiracles gradually shrinking.

Gnaptorina himalaya Shi, Ren & Merkl, 2007

Examined materials. Larvae. 2 exx. (MHBU): Garyü Countyside, Qusum County, Xizang/ 28°50.25' N, 91°59.90' E/ Alt. 4790m/ 2019-VII-31/ Xiu-Min Li leg.; 4 exx. (MHBU): Zag La, Comai County, Xizang/ 2019-VII-31/ Guo-Dong Ren leg.

Description. Body (Fig. 6A–C). Larvae length 16.8–22.0 mm, width 2.1–2.3 mm, thick. Body yellowish brown, shiny, body wall ossified; median line obvious on thorax dorsally and abdominal tergite I.

Head (Fig. 6B, D–G). Labrum transverse; apical part with six setae; anterior margin with two discal and six slender lateral marginal setae; epipharynx with sparse setae on lateral margin, with two basal spines on central area, between

the basal spines with four mastoids, with three pairs of mastoids above the basal spines; mandible left-right unsymmetrical, membranous elevation with two setae (Fig. 6D, F, G). Epicranial stem Y or V-shaped; frons convex, with sparse setae on lateral margins, with four pairs of setae at apex (a pair on anterior margin, a pair on middle margin, two pairs on posterior margin) (Fig. 6D, F). Ocelli evident, three parallel rows arranged transversely (Fig. 6B). Maxillary palpi (Fig. 6E) three-segmented, cylindrical, and conical at apex; I widest, II longest. Labial palps two-segmented, short; II conical; prementum shorter than mentum, with two setae on anterior margin, apex with two long setae; mentum convex, trapezoidal, base of mentum straight; mentum wide and short, posterior margin with 4–6 long setae; submentum with nine setae on middle margin. Antennae three-segmented, cylindrical at apex; I nearly as long as II; III shortest and narrowest (Fig. 6B, D–G).

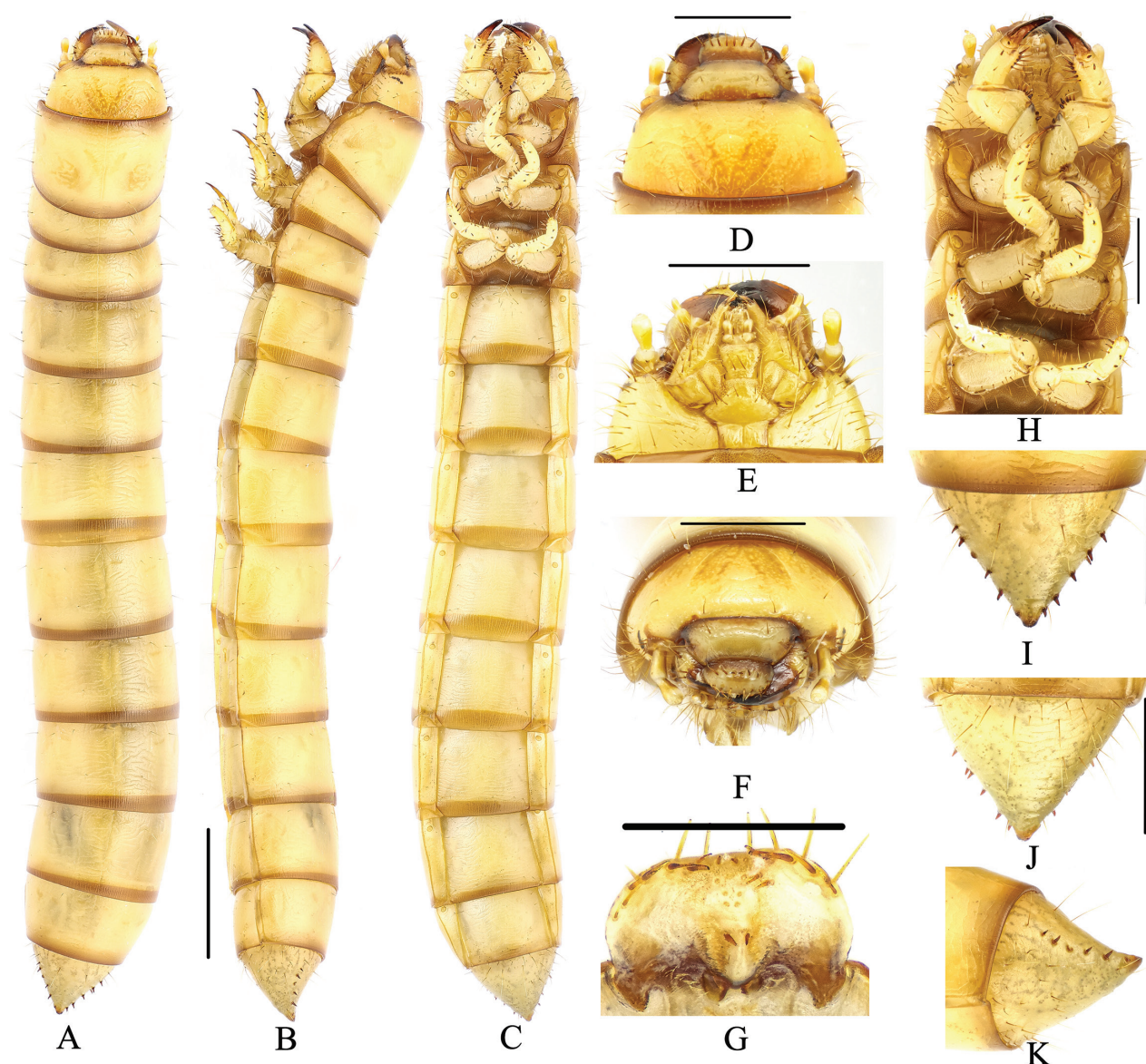


Figure 6. Larva of *Gnaptorina himalaya* Shi, Ren & Merkl, 2007 **A** habitus, dorsal view **B** habitus, lateral view **C** habitus, ventral view **D** head, dorsal view **E** head, ventral view **F** head, vertex view **G** epipharynx **H** legs **I** pygopods, dorsal view **J** pygopods, ventral view **K** pygopods, lateral view. Scale bars: 2 mm (**A–C**); 1 mm (**D–F, H–K**); 0.5 mm (**G**).

Thorax (Fig. 6A). Pronotum with four pairs of setae (two pairs of setae on anterior margin, a pair of setae on middle margin, a pair of setae on posterior margin); mesonotum with three pairs of long setae, a pair on anterior margin, two pairs on middle; metanotum with four pairs of setae, two pairs on anterior margin, two pairs on middle. Anterior and posterior borders of pronotum with brown longitudinal stripes, and a pair of pale brown irregular spots; posterior border of mesonotum and metanotum with a brown longitudinal stripe. Pronotum longest, $2.80 \times$ as long as mesonotum, $2.06 \times$ as long as metanotum, mesonotum shortest.

Legs (Fig. 6H). Protarsungulus with a strong, long seta on inner side and a strong, short spine on outer side at base. Profemora and protibiae gradually narrowing towards apex; inner margin setal formula of prothoracic leg 5(4): 6(2–3): 2(2); outer margin of tibiae with one strong seta and one short spine; outer margin of femora with two setae; trochanter with three setae. Mesotarsus with a strong, long seta on inner side and a strong, short spine on outer side at base; inner margin setal formula of mesothoracic leg 2–4(2–3): 5(2–3): 2(2); outer margin of tibiae with two spines; outer margin of femora with two spines; outer margin of trochanters with one spine and two setae. Metatarsus with two strong, short spines at base; inner margin setal formula of metathoracic leg 3(2–3): 4(2): 2(2), outer margin of tibiae with two spines, outer margin of femora with two spines, outer margin of trochanters with one spine and two setae.

Abdomen (Fig. 6A, C). Not constricted between VIII and IX segments. Approximately $3.91 \times$ as long as thorax; abdominal segments I–VIII subcylindrical, with transverses plicae; ventral side of abdominal segment I with 11 setae on anterior margin and 5–7 on each side, with two pairs of setae on posterior margin; ventral side of abdominal segment II with six pairs of setae (four pairs of setae on lateral margin, two pairs of setae on posterior margin); ventral side of abdominal segments III–VIII with four pairs of setae on lateral margin (two pairs of setae on mid-lateral margin, two pairs of setae on posterior margin). Last segment conical, $0.87 \times$ as long as VIII, distinctly narrower than VIII; last segment surface of convex disc with sparse long setae in ventral view, with a row of short spines each side (five spines on left, five spines on right); last segment dorsally flattened, urogomphi inconspicuous, with one short spines (Fig. 6I–K).

Spiracles (Fig. 6C). Lateral margins of abdominal segments I–VIII and mesothorax each with a pair of oval spiracles, mesothorax spiracles much larger than abdominal spiracles, abdominal segments I–VIII spiracles gradually shrinking.

***Gnaptorina kangmar* Shi, Ren & Merkl, 2007**

Examined materials. Larvae. 27 exx. (MHBU): Nai Chin Kangsang Snow Mountain, Xizang/ $28^{\circ}53.90' N$, $90^{\circ}09.85' E$ / Alt. 5030m/ 2014-VIII-6/ Guo-Dong Ren, Xing-Long Bai, Jun-Sheng Shan leg.; 21 exx. (MHBU): Gyangzê County, Xizang/ 2014-VIII-6/ Guo-Dong Ren, Xing-Long Bai, Jun-Sheng Shan leg.

Description. Body (Fig. 7A–C). Larvae length 19.2–20.0 mm, width 2.3–2.5 mm, moderately thickened. Body yellowish brown, shiny, body wall ossified; median line obvious on pronotum and mesonotum.

Head (Fig. 7B, D–G). Labrum transverse; apical part with six setae; anterior margin with two discal and six slender lateral marginal setae; epipharynx with sparse setae on lateral margin, with two basal spines on central area, between

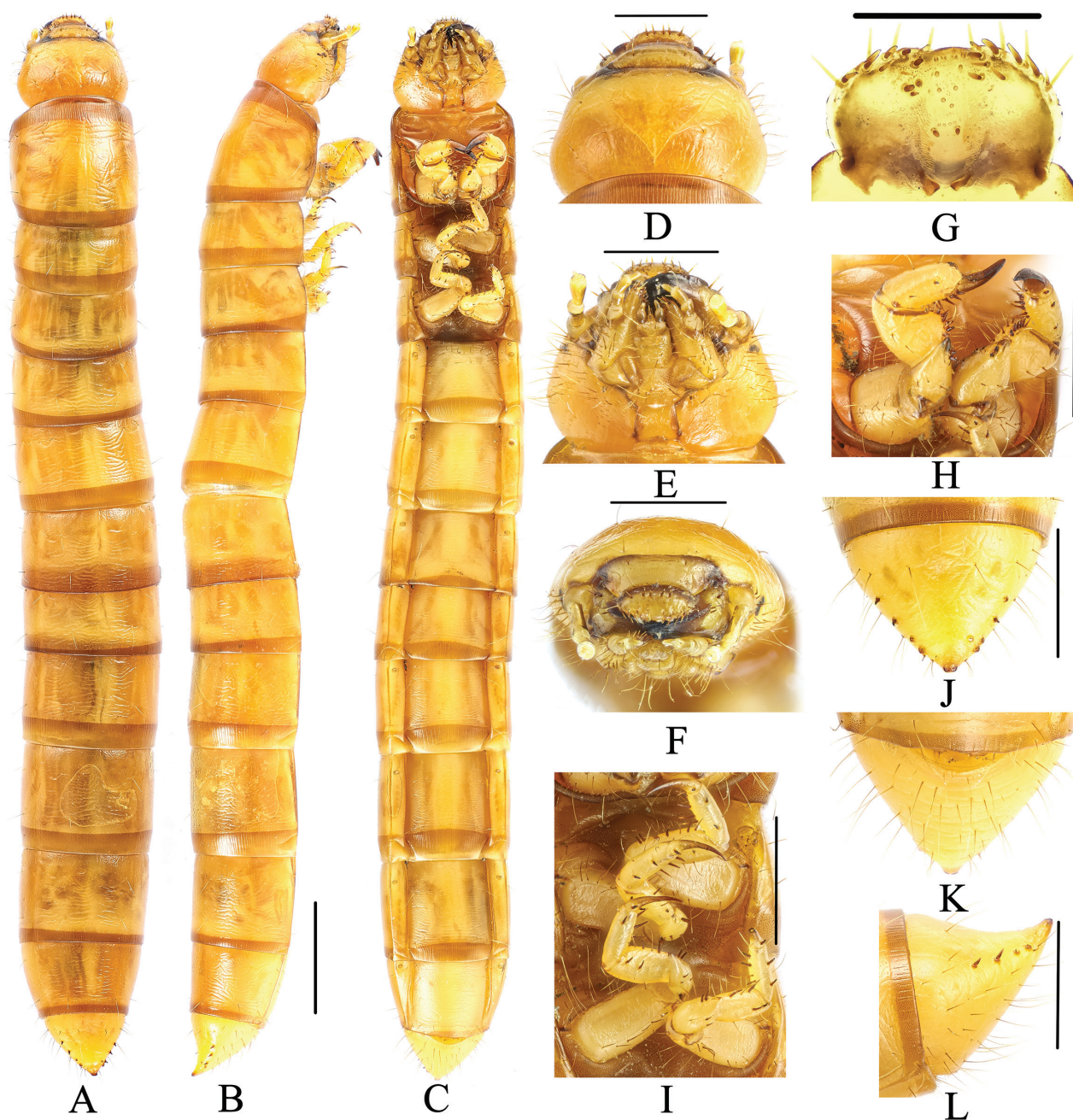


Figure 7. Larva of *Gnaptorina kangmar* Shi, Ren & Merkl, 2007 **A** habitus, dorsal view **B** habitus, lateral view **C** habitus, ventral view **D** head, dorsal view **E** head, ventral view **F** head, vertex view **G** epipharynx **H** prothoracic leg, lateral view **I** mesothoracic and metathoracic legs, lateral view **J** pygopods, dorsal view **K** pygopods, ventral view **L** pygopods, lateral view. Scale bars: 2 mm (**A–C**); 1 mm (**D–F, H–L**); 0.5 mm (**G**).

the basal spines with four mastoids, with six mastoids above the basal spines; mandible left-right unsymmetrical, membranous elevation with two setae (Fig. 7D, E, G). Epicranial stem Y-shaped; frons convex, with sparse setae on lateral margins, with four pairs of setae at apex (a pair on anterior margin, a pair on middle margin, two pairs on mid-posterior margin) (Fig. 7D, F). Ocelli evident, two parallel rows arranged transversely (Fig. 7B). Maxillary palpi (Fig. 7E) three-segmented, cylindrical, and conical at apex; I widest, II longest. Labial palps two-segmented, short; II conical; prementum short, with two setae on anterior margin, apex with two long setae; mentum convex, trapezoidal, base

of mentum straight; mentum wide and short, lateral margin with five or six long setae, mid-posterior margin with two long setae; submentum with nine setae on middle margin. Antennae three-segmented, cylindrical at apex; I longest; III shortest and narrowest (Fig. 7B, D–G).

Thorax (Fig. 7A). Pronotum and mesonotum with four pairs of setae (two pairs of setae on anterior margin, two pairs of setae on posterior margin); metanotum with three pairs of long setae, a pair on mid-anterior margin, two pairs on middle. Anterior and posterior borders of pronotum with brown longitudinal stripes; posterior border of mesonotum and metanotum with a brown longitudinal stripe. Pronotum longest, $2.03 \times$ as long as mesonotum, $1.89 \times$ as long as metanotum, mesonotum shortest.

Legs (Fig. 7H, I). Protarsungulus with a strong, long seta on inner side and a strong, short spine on outer side at base. Profemora and protibiae gradually narrowing towards apex; inner margin setal formula of prothoracic leg 5(1): 7(5–6): 2(2); outer margin of tibiae with two strong and short spines; outer margin of femora with two setae; trochanter with three setae. Mesotarsus with a strong, long seta on inner side and a strong, short spine on outer side at base; inner margin setal formula of mesothoracic leg 4(2): 4(2): 2(2); outer margin of tibiae with two spines; outer margin of femora with two spines; outer margin of trochanters with two spines and one seta (Fig. 7H). Metatarsus with a strong, long seta on inner side and a strong, short spine on outer side at base; inner margin setal formula of metathoracic leg 4(3): 5(2): 2(2), outer margin of tibiae with two spines, outer margin of femora with two spines, outer margin of trochanters with two spines and one seta.

Abdomen (Fig. 7A, C). Not constricted between VIII and IX segments. Approximately $2.68 \times$ as long as thorax; abdominal segments I–VIII subcylindrical, with transverses plicae; ventral side of abdominal segment I with 12 setae on anterior margin and six setae on each side, with two pairs of setae on posterior margin; ventral side of abdominal segment II with seven pairs of setae (five pairs of setae on lateral margin, two pairs of setae on posterior margin); ventral side of abdominal segments III–VIII with three pairs of setae (two pairs of setae on mid-lateral margin, a pair of setae on posterior margin); ventral side of abdominal segment VIII with four pairs of setae on lateral margin and two pairs of setae on posterior margin. Last segment conical, $0.91 \times$ as long as VIII, distinctly narrower than VIII; last segment surface of convex disc with sparse long setae in ventral view, with a row of short spines on each side (five spines on left, five spines on right); last segment dorsally flattened, urogomphi inconspicuous, with two short spines (Fig. 7J–L).

Spiracles (Fig. 7C). Lateral margins of abdominal segments I–VIII and mesothorax each with a pair of oval spiracles, mesothorax spiracles much larger than abdominal spiracles, abdominal segments I–VIII spiracles gradually shrinking.

Discussion

Molecular species identification has become an important approach in insect taxonomy (Tautz et al. 2002; Hebert et al. 2003; Meier et al. 2006; Rodriguez et al. 2022). These approaches are capable of establishing correlations between larval and adult stages through DNA sequences, and of providing valuable reference information for larval taxonomy (Kamiński et al. 2019). Most

Gnaptorina species are distributed in the high-elevation areas of the Qinghai-Xizang Plateau, where they usually have restricted areas of distribution (Bai et al. 2020; Li et al. 2021; Ji et al. 2024). Therefore, it is usually hard to obtain larvae and pupae through laboratory rearing because of the difficulty in replicating the natural conditions of *Gnaptorina* in the wild. In this study, the larval samples were directly collected from the field, whose classification is challenging due to the lack of larval information on the known species. Our results clearly provided a tool to help associate the larva with known or unknown adults, which successfully resolved the problem of larval taxonomic status. In addition, the results of molecular species delimitation are consistent with previous studies (Li et al. 2021). However, molecular species delimitation was performed based on 88 samples of 32 species (82% of the known species). We did not have a high number of specimens per species on average, which could lead to an increase in the number of inferred MOTUs. Yet molecular species delimitation was performed only based on COI gene fragments per species in this study, requiring a cautious approach to any taxonomic changes. For these taxa, we identified distinctive morphological characters that could support their status as separate species. The molecular phylogenetic results revealed that the larval specimens all belong to the subgenus *Hesperoptorina*. Before the present study, the larval information in only known for three species of the subgenus *Gnaptorina* (*Gnaptorina cylindricollis* Reitter, 1889, *Gnaptorina felicitana* Reitter, 1887, and *Gnaptorina lhorongica* Li, 2024) were recorded. The immature stages of more genera and species need to be properly documented in order to develop an applicable system of the larval and pupal taxonomy in the tribe Blaptini.

Acknowledgements

We would like to thank Prof. Jun-Xia Zhang and Dr. Zhao Pan (College of Life Sciences, Hebei University) for their valuable comments and corrections. We are also very grateful to the editor and anonymous reviewers for their constructive suggestions on the manuscript.

Additional information

Conflict of interest

The authors have declared that no competing interests exist.

Ethical statement

No ethical statement was reported.

Funding

This research was funded by the National Natural Science Foundation of China (32170477) and the Natural Science Foundation of Hebei (C2024201003).

Author contributions

Conceptualisation: B-YJ, X-ML and G-DR. Data curation: X-ML, M-CG and T-YG. Formal analysis: B-YJ, T-YG and X-ML. Writing-original draft: B-YJ and X-ML. Visualisation: B-YJ and T-YG. Funding acquisition: X-ML. Writing-review and editing: B-YJ and T-YG.

Author ORCIDs

Bao-Yue Ji  <https://orcid.org/0000-0002-9250-5481>

Tong-Yang Guo  <https://orcid.org/0009-0004-1880-7045>

Mei-Chang Gu  <https://orcid.org/0009-0003-6617-4572>

Guo-Dong Ren  <https://orcid.org/0000-0001-5808-9122>

Xiu-Min Li  <https://orcid.org/0000-0003-0575-1869>

Data availability

All of the data that support the findings of this study are available in the main text.

References

- Bai XL, Li XM, Ren GD (2020) Description of a new subgenus and four new species of *Gnaptorina* Reitter, 1887 (Coleoptera: Tenebrionidae: Blaptini) from China. *Zootaxa* 4809(1): 165–176. <https://doi.org/10.11646/zootaxa.4809.1.10>
- Bai XL, Liu JZ, Ren GD (2023) *Vihtagona vietnamensis*-Newly Recorded Genus and Species from China (Coleoptera: Tenebrionidae: Blaptini). *Sichuan Journal of Zoology* 42(6): 696–700. <http://dx.doi.org/10.11984/j.issn.1000-7083.20230051>
- Chigray IA (2019) A new genus and species of darkling beetles of the tribe Blaptini (Coleoptera: Tenebrionidae) from Afghanistan and taxonomic changes in the tribe. *Entomological Review* 99(7): 914–923. <https://doi.org/10.1134/S0013873819070054>
- Chigray IA, Kirejtshuk AG (2023) The supraspecific structure of the subtribe Blaptina Leach, 1815 (Coleoptera, Tenebrionidae: Blaptinae). *Acta Zoologica Academiae Scientiarum Hungaricae* 69(3): 213–245. <https://doi.org/10.17109/AZH.69.3.213.2023>
- Delicour S, Flot JF (2018) The hitchhiker's guide to single-locus species delimitation. *Molecular Ecology Resources* 18(6): 1234–1246. <https://doi.org/10.1111/1755-0998.12908>
- Folmer O, Black M, Hoeh W, Lutz R, Vrijenhoek R (1994) DNA primers for amplification of mitochondrial cytochrome c oxidase subunit I from diverse metazoan invertebrates. *Molecular Marine Biology and Biotechnology* 3: 294–299.
- Grebennikov VV, Scholtz CH (2004) The basal phylogeny of Scarabaeoidea (Insecta: Coleoptera) inferred from larval morphology. *Invertebrate Systematics* 18(3): 321–348. <https://doi.org/10.1071/IS03013>
- Hebert PDN, Cywinska A, Ball SL, Dewaard JR (2003) Biological identifications through DNA barcodes. *Proceedings of the Royal Society B, Biological Sciences* 270(1512): 313–321. <https://doi.org/10.1098/rspb.2002.2218>
- Iwan D, Löbl I (2020) Tenebrionoidea. *Catalogue of Palaearctic Coleoptera* [M]. Volume 5. Koninklijke Brill NV, Leiden, The Netherlands, 945 pp. https://doi.org/10.1163/9789004434998_004
- Ji BY, Ma XT, Rong JD, Ren GD, Pan Z, Li XM (2024) The adult, pupa, and larva of a new species of *Gnaptorina* Reitter, 1887 (Coleoptera, Tenebrionidae, Blaptini) from the Tibetan Plateau, with molecular phylogenetic inferences. *ZooKeys* 1190: 91–106. <https://doi.org/10.3897/zookeys.1190.113126>
- Kamiński MJ, Lumen R, Kubicz Jr M, Steiner Jr W, Kanda K, Iwan D (2019) Immature stages of beetles representing the 'Opatrinoid' clade (Coleoptera: Tenebrionidae): an overview of current knowledge of the larval morphology and some resulting taxonomic notes on Blapstinina. *Zoomorphology* 138(3): 349–370. <https://doi.org/10.1007/s00435-019-00443-7>

- Kamiński MJ, Lumen R, Kanda K, Iwan D, Johnston MA, Kergoat GJ, Bouchard P, Bai XL, Li XM, Ren GD, Smith AD (2021) Reevaluation of Blapimorpha and Opatrinae: addressing a major phylogeny-classification gap in darkling beetles (Coleoptera: Tenebrionidae: Blaptinae). *Systematic Entomology* 46(1): 140–156. <https://doi.org/10.1111/syen.12453>
- Lawrence JF, Seago AE, Newton AF, Thayer MK, Marvaldi AE, Slipinski A (2011) Phylogeny of the Coleoptera based on morphological characters of adults and larvae. *Annales Zoologici* 61(1): 1–217. <https://doi.org/10.3161/000345411X576725>
- Li XM, Bai XL, Ren GD (2018) A new species of the genus *Blaptogonia* from the Himalayas with four DNA markers (Coleoptera, Tenebrionidae, Blaptini). *ZooKeys* 773: 69–78. <https://doi.org/10.3897/zookeys.773.24656>
- Li XM, Bai XL, Ren GD (2019) Two new species of the genus *Gnaptorina* Reitter from the Hengduan Mountains, China (Coleoptera: Tenebrionidae: Blaptini). *Zootaxa* 4695(1): 83–89. <https://doi.org/10.11646/zootaxa.4695.1>
- Li XM, Bai XL, Kergoat GJ, Pan Z, Ren GD (2021) Phylogenetics, historical biogeography and molecular species delimitation of *Gnaptorina* Reitter (Coleoptera: Tenebrionidae: Blaptini). *Systematic Entomology* 46(1): 239–251. <https://doi.org/10.1111/syen.12459>
- Luo A, Ling C, Ho SYW, Zhu CD (2018) Comparison of methods for molecular species delimitation across a range of speciation scenarios. *Systematic Biology* 67(5): 830–846. <https://doi.org/10.1093/sysbio/syy011>
- Medvedev GS (2004) New species of the darkling-beetle tribe Blaptini (Coleoptera, Tenebrionidae) from India, Nepal and China. *Entomologicheskoe Obozrenie* 83: 163–189. [In Russian, English translation: *Entomological Review* 84: 78–99]
- Medvedev GS (2006) To the systematics and nomenclature of tenebrionid beetles of the tribes Phaleriini, Lachnogyini, Klewariini, and Blaptini (Coleoptera, Tenebrionidae). *Entomological Review* 86(7): 820–839. <https://doi.org/10.1134/S0013873806070062>
- Medvedev GS (2009) Composition of the genera *Gnaptorina* Reitter and *Pseudognaptorina* Kaszab of the tribe Blaptini (Coleoptera, Tenebrionidae). *Entomological Review* 89(4): 451–461. <https://doi.org/10.1134/S0013873809040095>
- Medvedev GS, Merkl O (2002) *Vihtagona vietnamensis* Gen. Et Sp. N. From Vietnam (Coleoptera, Tenebrionidae: Blaptini). *Acta Zoologica Academiae Scientiarum Hungaricae* 48(4): 317–332.
- Meier R, Shiyang K, Vaidya G, Ng PKL (2006) DNA barcoding and taxonomy in Diptera: A tale of high intraspecific variability and low identification success. *Systematic Biology* 55(5): 715–728. <https://doi.org/10.1080/10635150600969864>
- Minh BQ, Nguyen MAT, Von Haeseler A (2013) Ultrafast approximation for phylogenetic bootstrap. *Molecular Biology and Evolution* 30(5): 1188–1195. <https://doi.org/10.1093/molbev/mst024>
- Nguyen LT, Schmidt HA, Von Haeseler A, Minh BQ (2015) IQ-TREE: A fast and effective stochastic algorithm for estimating maximum-likelihood phylogenies. *Molecular Biology and Evolution* 32(1): 268–274. <https://doi.org/10.1093/molbev/msu300>
- Pons J, Barraclough TG, Gomez-Zurita J, Cardoso A, Duran DP, Hazell S, Kamoun S, Sumlin WD, Vogler AP (2006) Sequence based species delimitation for the DNA taxonomy of undescribed insects. *Systematic Biology* 55(4): 595–609. <https://doi.org/10.1080/10635150600852011>
- Puillandre N, Brouillet S, Achaz G (2021) ASAP: Assemble species by automatic partitioning. *Molecular Ecology Resources* 21(2): 609–620. <https://doi.org/10.1111/1755-0998.13281>

- Ren GD, Ba YB, Liu HY, Niu YP, Zhu XC, Li Z, Shi AM (2016) Coleoptera: Tenebrionidae (I); Fauna Sinica: Insecta, Volume 63. Science Press, Beijing, 532 pp.
- Rodriguez EJ, Steck GJ, Moore MR, Norrbom AL, Diaz J, Somma LA, Ruiz-Arce R, Sutton BD, Nolzco N, Muller A, Branham MA (2022) Exceptional larval morphology of nine species of the *Anastrepha mucronota* speciesgroup (Diptera, Tephritidae). *ZooKeys* 1127: 155–215. <https://doi.org/10.3897/zookeys.1127.84628>
- Skopin NG (1960) Material on the morphology and the ecology of larvae of the tribe Blaptini (Coleoptera, Tenebrionidae). *Trudy Instituta zoologii Akademii nauk Kazakhskoy SSR* 11: 36–71. [In Russian]
- Tautz D, Arctander P, Minelli A, Thomas RH, Vogler AP (2002) DNA points the way ahead in taxonomy. *Nature* 418(6897): 479–479. <https://doi.org/10.1038/418479a>
- Yu YZ, Ren GD, Sun QX (1996) Morphology and genus and species key of common Blaptini larvae in Northern China. *Entomological Knowledge* 4: 198–203.
- Yu YZ, Zhang DZ, Wang XP (1999) The larval morphology of five species of the Blaptini-Tribe (Coleoptera: Tenebrionidea). *Journal of Ningxia Agricultural College* 4: 15–20.
- Zhang JJ, Kapli P, Pavlidis P, Stamatakis A (2013) A general species delimitation method with applications to phylogenetic placements. *Bioinformatics (Oxford, England)* 29(22): 2869–2876. <https://doi.org/10.1093/bioinformatics/btt499>
- Zhang D, Gao FL, Jakovlić I, Zou H, Zhang J, Li WX, Wang GT (2020) PhyloSuite: An integrated and scalable desktop platform for streamlined molecular sequence data management and evolutionary phylogenetics studies. *Molecular Ecology Resources* 20(1): 348–355. <https://doi.org/10.1111/1755-0998.13096>
- Zhu XC, Ren GD (2014) The larvae of *Gnaptorina felicitana* and *Agnaptoria amdoensis* of the tribe Blaptini from China (Coleoptera:Tenebrionidae). *Zoological Systematics* 39(02): 275–282.